IL NUOVO CIMENTO **40 C** (2017) 4
DOI 10.1393/ncc/i2017-17004-y

COLLOQUIA: IFAE 2016

Recent results on the Higgs boson from the LHC

R. COVARELLI for the ATLAS and CMS COLLABORATIONS
Università di Torino and Sezione INFN di Torino - Torino, Italy

received 17 October 2016

Summary. — An overview of recent ATLAS and CMS results on the Standard-Model Higgs boson properties will be presented, with particular focus on preliminary property measurements performed using up to 3.2 fb^{-1} data collected in 2015 at the center-of-mass energy of 13 TeV.

1. – Introduction

The precise determination of the Higgs-boson mass performed by the ATLAS and CMS collaborations strongly constrains the theoretical expectations for a Standard-Model (SM) Higgs boson and opens possibilities for precision data/theory comparisons of its properties. In view of such accurate experimental measurements, inclusive analyses are progressively replaced by searches in the various modes of production (by means of separate studies or event categorization), which allow selection of purer event samples and measurements of couplings to fermions and vector bosons.

Using 2.4 to 3.2 fb^{-1} data luminosity collected in 2015 at the center-of-mass energy of 13 TeV, the ATLAS and CMS experiments have already performed preliminary measurements of the SM Higgs boson properties. A review of such results is presented, comparing them with the well-established high-statistics results of the first LHC run at 7–8 TeV.

2. – State of the art after Run1

2˙1. *Higgs boson mass.* – The Higgs boson mass has been measured precisely by both experiments using the $H \to ZZ^* \to 4\ell$ and $H \to \gamma\gamma$ channels, which have a typical mass resolution of 1–2%. The main systematic uncertainty is the lepton momentum calibration in $H \to ZZ^* \to 4\ell$, while for $H \to \gamma\gamma$ there are large contributions from the electromagnetic calorimeter response (non-linearity, lateral shower shape, calibration with $Z \to e^+e^-$ etc.) and from the estimate of the material budget in front of the calorimeter.

A good compatibility between channels and experiments is observed and the combined mass measurement is $m_H = (125.09 \pm 0.21_{\text{stat.}} \pm 0.11_{\text{syst.}})$ GeV [1]. SM expectations for all the quantities entering the combined measurement in the two experiments are therefore calculated at this mass value.

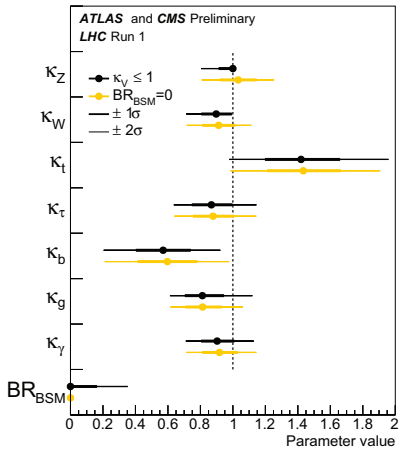

Fig. 1. – Fit results for the two parameterisations allowing BSM loop couplings, with $\kappa_W, \kappa_Z \leq 1$ or without additional BSM contributions to the Higgs boson width, *i.e.* $\mathrm{BR_{BSM}} = 0$ [2]. The measured results for the combination of ATLAS and CMS are reported together with their uncertainties. The error bars indicate the 1σ (thick lines) and 2σ (thin lines) intervals.

2˙2. *Constraints on coupling deviations.* – In the formalism used in the ATLAS-CMS Higgs-boson property combination, $\sigma \cdot$ BR quantities are computed by scaling the couplings of the Higgs boson to other SM particles with free parameters $\kappa = g/g_{SM}$. Most cross sections and partial widths depend on the corresponding value of κ^2, but not all: for example the interference of t-quark and W loops in the $H \to \gamma\gamma$ decay brings a more complex combination of κ parameters.

Even in the most general New Physics scenarios, assumptions about Γ_H are required, because this parameter is not measured. Two scenarios are considered: one in which the sum of partial widths is bound to the SM total width and one where beyond-Standard-Model (BSM) decays are permitted, but with a constraint on $\kappa_W, \kappa_Z \leq 1$. Such assumptions are valid in a broad range of BSM theories. Figure 1 shows constraints on couplings from combined ATLAS and CMS Run1 results in these two scenarios [2].

Scenarios with more restrictive constraints dedicated to specific classes of BSM theories are also considered, like common scale factors for all fermions and bosons (κ_f, κ_V).

2˙3. *Spin and differential distributions.* – Hypotheses of spin-parity alternatives (0^-, 1, 2^+_m, 2^+_h, 2^- etc.) are largely disfavored by ATLAS and CMS measurements combining the channels $H \to ZZ^* \to 4\ell$, $H \to \gamma\gamma$ and $H \to WW^* \to 2\ell 2\nu$. Accurate analyses of the "tensor structure" of HVV couplings in CMS (*i.e.* parametrizing them with effective New Physics parameters that would induce pseudoscalar, tensor components etc.) [3] have led to an upper limit on the effective pseudoscalar cross-section fraction of $f_{a3}^{ZZ} < 0.0034$ at 95% Confidence Level (CL). Differential distributions in ATLAS using the $H \to ZZ^* \to 4\ell$ and $H \to \gamma\gamma$ channels [4] show small discrepancies with resummed NNLO+NNLL QCD results, which are still not conclusive.

2˙4. *$t\bar{t}H$ and HH.* – The rare HH (double Higgs production) and $t\bar{t}H$ (Higgs boson production in association to a $t\bar{t}$ quark pair) channels are interesting because they give unique access to the scaling parameters κ_H (Higgs self-coupling) and κ_t, respectively.

For $t\bar{t}H$, different exclusive (like $H \to b\bar{b}$) or semi-exclusive (like multi-leptonic) decay

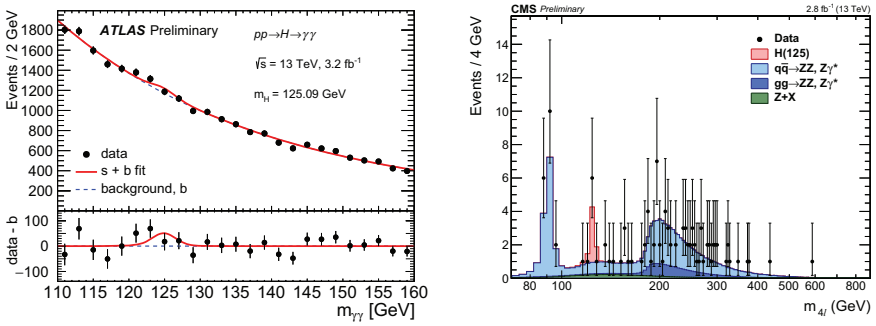

Fig. 2. – Left: Diphoton invariant-mass spectrum observed in the 13 TeV ATLAS data [9]. The solid red curve shows the fitted signal plus background model when the Higgs boson mass is fixed at 125.09 GeV. The background component of the fit is shown with the dotted blue curve. The bottom plot shows the distribution of the background-subtracted data. Right: Distribution of the four-lepton invariant mass in CMS [12]. Stacked histograms represent expected distributions: the 125 GeV Higgs boson signal and the ZZ backgrounds are normalized to the SM expectation, while other backgrounds are estimated using data control regions.

channels are used. In Run1 combinations, CMS reports a slight excess ($\mu = \sigma/\sigma_{SM} = 2.8 \pm 1.0$) dominated by yields in final states with 2 or 3 leptons [5]. ATLAS updated combined results very recently, by adding $t\bar{t}H$, $H \to b\bar{b}$ in a completely hadronic final state [6]. This final state has the highest branching ratio but a very low purity, needing a complex data-derived estimate of the multi-jet background.

SM HH production is not yet detectable. However, production rates are increased in various BSM models, both in resonant (G^*_{KK}, radion, heavy $H^0 \to HH$) and non-resonant form. Several analyses in ATLAS and CMS seek to exploit channels with high BR ($b\bar{b}b\bar{b}$, $b\bar{b}\tau^+\tau^-$) or clean ($b\bar{b}\gamma\gamma$, $WW^*\gamma\gamma$) in various mass ranges [7,8]. The combined limit on the non-resonant cross-section from ATLAS is $\sigma_{HH} < 63\,\sigma^{SM}_{HH}$ at the 95% CL.

3. – First results of Run2

3˙1. $H \to \gamma\gamma$. – The key points of the $H \to \gamma\gamma$ searches are the optimal energy resolution and photon selection. The ATLAS analysis [9] only targets an inclusive cross-section measurement and uses a cut-based approach for this selection, while CMS [10] has a multivariate approach and various signal categories for a measurement of the signal strength in different production modes. The variables used are based on the shape and the expected containment of the showers, track and calorimeter isolation, and the rejection of π^0.

Another important aspect of the diphoton mass reconstruction is the identification of the primary vertex, where CMS adopts a multivariate analysis using the Σp_T^2 of tracks in the vertex and their balancing w.r.t. the diphoton system and ATLAS uses a similar technique but including photon trajectory estimates from the pointing calorimeter. Both experiments fit the distribution of $m_{\gamma\gamma}$ in signal categories of different purity. Figure 2 (left) shows the inclusive distribution as observed in ATLAS 13 TeV data.

CMS results are given in terms of Higgs-boson signal strength: the inclusive result is $\mu = \sigma/\sigma_{SM} = 0.69^{+0.47}_{-0.42}$ and for all categories the result is compatible with SM expectation. ATLAS measures the fiducial cross section in a fiducial detector region, obtaining $\sigma_{\text{fid.}} = (52 \pm 34_{\text{stat.}}\ ^{+21}_{-13\,\text{syst.}} \pm 3_{\text{lumi.}})$ fb.

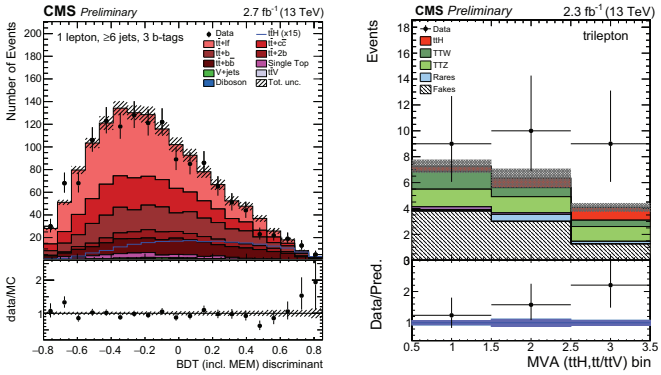

Fig. 3. – Left: BDT shapes in the $t\bar{t}H$, $H \to b\bar{b}$ semileptonic channel, (≥ 6 jets, 3 b-tags) category with high BDT output, after the fit to data [14]. The expected background contributions (filled histograms) are stacked, and the expected signal distribution for a Higgs-boson mass of 125 GeV is superimposed. Each contribution is normalized to the data integrated luminosity, and the signal contribution is additionally scaled by a factor of 15. Right: BDT kinematic discriminants in the bins used for signal extraction, for the three-lepton channel of the multi-leptonic $t\bar{t}H$ analysis [15]. Pre-fit distributions are shown. Uncertainties are statistical only.

3˙2. $H \to ZZ^* \to 4\ell$. – The crucial aspect in $H \to ZZ^* \to 4\ell$ searches is the selection of high-quality leptons, including final-state-radiation recovery, with a high efficiency. Estimate of the backgrounds is based on theory and Monte Carlo simulation for the $ZZ^{(*)}$ and from control region in data for reducible (mainly $Z+X$) backgrounds. Figure 2 (right) shows the $m_{4\ell}$ distribution as observed in CMS 13 TeV data.

The signal extraction in ATLAS [11] is performed via a fit to the $m_{4\ell}$ distribution after a kinematic fit with a constrained Z mass. In CMS [12], two signal categories are defined (tagged as Vector-Boson Fusion, "VBF-tagged", and other events) and the bare $m_{4\ell}$ plus a matrix-element-based kinematic discriminant are used as analysis variables. However, due to the limited statistics, only one and zero events, respectively, are observed in ATLAS and CMS with characteristics compatible with VBF production.

CMS reports a global signal strength of $\mu = 0.89^{+0.62}_{-0.46}$ and a fiducial cross section of $\sigma_{\text{fid.}} = (2.48\ ^{+1.48}_{-1.14\,\text{stat+syst.}}\ ^{+0.01}_{-0.04\,\text{model dep.}})$ fb, in very good agreement with the SM expectation. The combined $H \to \gamma\gamma$ and $H \to ZZ^* \to 4\ell$ result in ATLAS for the cross section extrapolated to the full phase space [13] is $\sigma = (24\ ^{+20}_{-17\,\text{syst.}}\ ^{+7}_{-3\,\text{syst.}})$ pb and is compatible with the SM expectation at the 1.3σ level.

3˙3. *$t\bar{t}H$ and HH.* – CMS has updated both the $t\bar{t}H$, $H \to b\bar{b}$ and multi-leptonic $t\bar{t}H$ analyses at 13 TeV [14, 15].

The former is a very complex channel with a dominant background of $t\bar{t}$ + jets (especially $t\bar{t} + b\bar{b}$, which has large theoretical uncertainties). The limited resolution of the reconstructed Higgs mass and the large jet combinatorics are also challenges for this measurement. There are two main analysis categories: the dileptonic one, selecting 2ℓ, 3 or more jets of which ≥ 2 b-tagged; and the semileptonic one, with 1ℓ, 4 or more jets of which ≥ 2 b-tagged. Additional classification is made based on number of jets, b-tagged jets and large $b\bar{b}$ momentum, for a total of 13 exclusive categories. Selection is performed based on a boosted decision tree (BDT), a BDT including the matrix-element method (MEM), or the MEM alone, depending on the reconstructed topology. A category with

boosted top quarks and Higgs boson is also exploited for the first time. Figure 3 (left) shows the output variable of the BDT in one of the most sensitive signal categories.

The multi-lepton analysis includes several possible Higgs decay modes ($H \to WW^*$, $H \to \tau^+\tau^-$, $H \to ZZ^*$, with subsequent leptonic decays). The dominant backgrounds are $t\bar{t}$ + jets with fake leptons and $t\bar{t}V$ events. The selection uses special identification methods to reduce the background from non-prompt leptons and signal categories take into account the number of leptons, as well as their total charge and the presence of an hadronic τ object. Figure 3 (right) shows the output variable of one of the BDT used for signal selection.

The observed signal strengths for $t\bar{t}H$ in CMS Run2 data are: $\mu = -2.0 \pm 1.8$ for $t\bar{t}H$, $H \to b\bar{b}$, $\mu = 0.6^{+1.4}_{-1.1}$ for $t\bar{t}H$ multi-leptonic, and $\mu = 3.8^{+4.5}_{-2.6}$ for $t\bar{t}H$, $H \to \gamma\gamma$, which is part of the inclusive analysis [10]. The combined result of those is $\mu = 0.15^{+0.95}_{-0.81}$. It is important to notice that, in spite of the limited statistics, the uncertanties in these measurements are approaching those of Run1, because of the $t\bar{t}H$ cross section increasing with $\sqrt{s}$ faster than other Higgs production modes.

Double-Higgs production has been searched for of in $b\bar{b}b\bar{b}$ channels (ATLAS / CMS), $b\bar{b}\gamma\gamma$ (ATLAS), and $b\bar{b}\tau^+\tau^-$ (CMS) [16, 17]. Exclusion limits for high-mass resonances are similar than those set in Run1, with $b\bar{b}b\bar{b}$ covering a wider mass, using merged jets. The limits on the non-resonant cross-section from ATLAS are $\sigma_{HH} < 96\ (102)\,\sigma^{SM}_{HH}$ at the 95% CL, in the $b\bar{b}b\bar{b}$ ($b\bar{b}\gamma\gamma$) channel, while CMS reports $\sigma_{HH} < 192\,\sigma^{SM}_{HH}$ at the 95% CL, in the $b\bar{b}\tau^+\tau^-$ final state.

REFERENCES

[1] ATLAS and CMS Collaborations, *Phys. Rev. Lett.*, **114** (2015) 191803.
[2] ATLAS and CMS Collaborations, ATLAS-CONF-2015-044, CMS-PAS-HIG-15-002.
[3] CMS Collaboration, *Phys. Rev. Lett.*, **115** (2015) 091801.
[4] ATLAS Collaboration, arXiv:1602.04305.
[5] CMS Collaboration, *JHEP*, **09** (2014) 087.
[6] ATLAS Collaboration, *JHEP*, **05** (2016) 160.
[7] ATLAS Collaboration, *Phys. Rev. D*, **92** (2015) 092004.
[8] CMS Collaboration, CMS-PAS-HIG-15-013.
[9] ATLAS Collaboration, ATLAS-CONF-2015-060.
[10] CMS Collaboration, CMS-PAS-HIG-15-005.
[11] ATLAS Collaboration, ATLAS-CONF-2015-050.
[12] CMS Collaboration, CMS-PAS-HIG-15-004.
[13] ATLAS Collaboration, ATLAS-CONF-2015-069.
[14] CMS Collaboration, CMS-PAS-HIG-16-004.
[15] CMS Collaboration, CMS-PAS-HIG-15-008.
[16] ATLAS Collaboration, ATLAS-CONF-2016-004, ATLAS-CONF-2016-017.
[17] CMS Collaboration, CMS-PAS-HIG-16-002, CMS-PAS-HIG-16-012.